AIAA JOURNAL
Vol. 38, No. 4, April 2000

Turbulence Generation in Homogeneous Particle-Laden Flows

J.-H. Chen,* J.-S. Wu,† and G. M. Faeth‡
University of Michigan, Ann Arbor, Michigan 48109-2140

The generation of turbulence by uniform fluxes of monodisperse spherical particles moving through a uniform flowing gas was studied experimentally. Phase velocities, moments, probability density functions, and energy spectra were measured within a counterflowing particle/gas wind tunnel using phase-discriminating laser velocimetry. Test conditions included particle Reynolds numbers of 106–990, particle volume fractions less than 0.003%, direct rates of dissipation of turbulence by particles less than 4%, and turbulence generation rates sufficient to yield relative turbulence intensities in the range 0.2–5.0%. Velocity records showed that the flow consisted of randomly arriving wake disturbances within a turbulent interwake region and that the particle wake properties corresponded to recent observations of laminarlike turbulent wakes for spheres at intermediate Reynolds numbers in turbulent environments. Probability density functions of velocities were peaked for streamwise velocities due to contributions from mean streamwise velocities in particle wakes but were Gaussian for cross stream velocities that only involve contributions from the turbulence in the wakes. Relative intensities of streamwise and cross stream velocity fluctuations were roughly correlated in terms of a dimensionless rate of turbulence dissipation factor. Finally, energy spectra exhibited prominent -1 and $-\frac{5}{3}$ power decay regions associated with contributions from mean velocities in particle wakes and particle and interwake turbulence, respectively.

Nomenclature

C_D = sphere drag coefficient
D = dissipation factor, $\varepsilon d_p C_D^{1/3}/(2U_p^3)$
d_p = sphere diameter
$E_u(k)$ = streamwise energy spectra
f = frequency
k = wave number, $2\pi f/\bar{u}$
L_u = streamwise integral length scale
ℓ_K = Kolmogorov length scale
ℓ_p = mean particle spacing
$\dot{n}''$ = particle number flux
Re = particle Reynolds number, $d_p U_p/\nu$
t_K = Kolmogorov timescale
U_p = mean streamwise relative velocity of a particle
u = streamwise gas velocity
u_K = Kolmogorov velocity scale
v = cross stream gas velocity
x = distance in direction of particle motion
ε = rate of dissipation of turbulence kinetic energy
ν = kinematic viscosity

Superscripts

$(\bar{\ })$ = mean value
$(\bar{\ })'$ = rms fluctuating value
$(\bar{\ })'^2$ = mean square fluctuating value

Introduction

A STUDY of the modification of continuous-phase turbulence properties due to the presence and motion of a dispersed phase is described. Hinze[1] identifies several turbulence modification mechanisms that are observed in dispersed-multiphase flows. Of these, the least understood involve direct effects of dispersed phases on continuous-phase turbulence properties, as follows: the exchange of kinetic energy between the dispersed and continuous phases as the dispersed-phase motion accommodates to the continuous-phase motion, denoted turbulence modulation, which generally decreases turbulence fluctuations,[2–4] and the direct disturbance of the continuous-phase velocity field by particle wakes, denoted turbulence generation, which generally increases turbulence fluctuations.[3–7] Evaluating the relative magnitude of these two effects has been addressed by a number of investigators.[2,8–11] These studies show that turbulence generation (modulation) dominates turbulence modification, tending to increase (decrease) turbulence levels, when dispersed-phase elements have large (small) relaxation times compared to characteristic turbulence timescales. As a result, turbulence generation dominates turbulence modification in many practical dispersed-multiphase flows having significant separated-flow effects, for example, sprays, particle-laden jets, bubbly jets, rainstorms, etc.

Past studies of turbulence generation have considered dilute dispersed-multiphase flows in both shear[3–5,11] and homogeneous[6,7,12] flow configurations; however, the latter are preferred because they avoid problems of separating turbulence generation from conventional turbulence production in shear flows. Lance and Bataille[12] report an early study of homogeneous air/water bubbly flows downstream of a turbulence-generating grid. Effects of turbulence generation caused a progressive increase of continuous-phase turbulence levels with increasing void fractions; unfortunately, these results are difficult to interpret due to combined effects of bubble- and grid-generated turbulence.

Earlier studies of homogeneous flows where turbulence generation was the only mechanism of turbulence production involved uniform number fluxes of nearly monodisperse beads falling at their terminal velocities in nearly stagnant (in the mean) water and air.[6,7] Measurements included phase velocities and turbulence properties for various particle number fluxes and particle sizes corresponding to intermediate Reynolds number conditions ($Re = 100$–800) that are typical of practical sprays. The flows were analyzed using a simplified stochastic method involving superposition of randomly arriving particle velocity fields, by extending the method Rice[13] used to analyze noise. The stochastic approach provided some useful interpretations of flow properties, but was problematical because information about particle wakes at intermediate Reynolds numbers in turbulent environments typical of homogenous dispersed flows was limited. Thus, wake properties were estimated by extrapolating available results at large Reynolds numbers in nonturbulent

Presented as Paper 98-0240 at the AIAA 36th Aerospace Sciences Meeting, Reno, NV, 12–15 January 1998; received 10 September 1998; revision received 10 May 1999; accepted for publication 14 September 1999.

*Graduate Student Research Assistant, Department of Aerospace Engineering; currently Postdoctoral Fellow, Department of Mechanical Engineering, University of Maryland, College Park, MD 20742.

†Research Fellow, Department of Aerospace Engineering; currently Assistant Professor, Department of Mechanical Engineering, National Chiao-Tung University, Hsin-Chu 30050, Taiwan, Republic of China.

‡A.B. Modine Professor, Department of Aerospace Engineering, 3000 François-Xavier Bagnoud Building, 1320 Beal Avenue. Fellow AIAA.

environments, which is questionable and caused convergence problems for the Rice[13] approach similar to those encountered during stochastic analysis of sedimentation.[14] Other questions about the approximate analysis of Refs. 6 and 7 concerned the extent that particle wakes interacted with each other and the nature of the flowfield between wakes (the interwake region) if wake-to-wake interactions were small. These studies were also problematical because the nearly stagnant (in the mean) continuous phases caused large experimental uncertainties due to large turbulence intensities (up to 1000%).

Subsequent studies of sphere wakes at intermediate Reynolds numbers in both nonturbulent and turbulent environments provided information needed to understand turbulence generation better.[15–17] Wakes in nonturbulent environments yielded anticipated behavior for self-preserving turbulent and laminar wakes.[18,19] Findings more relevant to turbulence generation involved sphere wakes at intermediate Reynolds numbers in turbulent (roughly isotropic) environments that showed that these wakes scaled similar to self-preserving laminar wakes but with enhanced viscosities due to the presence of turbulence (termed laminarlike turbulent wakes).[16,17] Naturally, the laminarlike turbulent wakes differed considerably from the wakes assumed during the earlier turbulence-generation studies.[6,7] Estimates of flow properties also suggested that the probability of direct wake-to-wake interactions was small; instead, it was likely that wake disturbances were imbedded in relatively large turbulent interwake regions. Whether laminarlike turbulent wakes actually were observed during turbulence-generation processes was still an issue, however, because such turbulence fields differ from the conventional isotropic turbulence that was considered in Refs. 16 and 17.

Past studies raise several questions about turbulence generation: Were wake disturbances during turbulence generation equivalent to the laminarlike turbulent wakes observed in Refs. 16 and 17, does the flow involve wake disturbances imbedded in a turbulent interwake region or does it involve strongly interacting wakes, and can turbulence generation properties measured at large turbulence intensities be confirmed for moderate turbulence intensities where experimental uncertainties are much reduced? These issues were addressed during this investigation, which had the following specific objectives: 1) measure stationary homogeneous dispersed flows involving nearly monodisperse spherical solid (glass) particles at intermediate Reynolds numbers in air, using a counterflow particle/air wind tunnel, 2) use the measurements to determine the nature of wake disturbances and wake-to-wake interactions during turbulence generation, and 3) use the measurements to highlight differences between turbulence fields associated with turbulence generation and more conventional turbulence. The present description of the study is brief, see Ref. 20 for more details and a complete tabulation of data.

Experimental Methods

The apparatus consisted of a vertical counterflow wind tunnel with upflowing air moving toward the suction side of a blower and freely falling particles introduced at the top of the apparatus using a particle feeder (Fig. 1). The airflow system consisted of a rounded inlet, a honeycomb flow straightener (10-mm hexagonal cells, 76 mm long) and a 16:1 contraction ratio to the 305 × 305 mm cross section windowed test section. The particle dispersion section was located just above the test section. The upper part of the particle dispersion section involved nine equally spaced screens (square pattern with 0.9-mm-diam wires spaced 4.2 mm apart) to disperse the particles and to achieve a uniform particle flux. This was followed by a honeycomb flow straightener (10-mm hexagonal cells, 76 mm long) to remove lateral particle motion caused by the screens. The particle inlet section and the transition section to the blower were at the upper end of the wind tunnel. The wind-tunnel airflow was provided by a single inlet variable speed blower. The particle flow was provided by a variable-speed screw feeder (Accurate, Model 310/04). After passing through the wind tunnel, the particles impacted on a plastic sheet within a particle collector. Microscope inspection showed that the particles were not damaged by passing through the wind tunnel; therefore, they were reused.

Measurements included particle number fluxes and gas and particle velocities. Particle number fluxes were measured by collecting

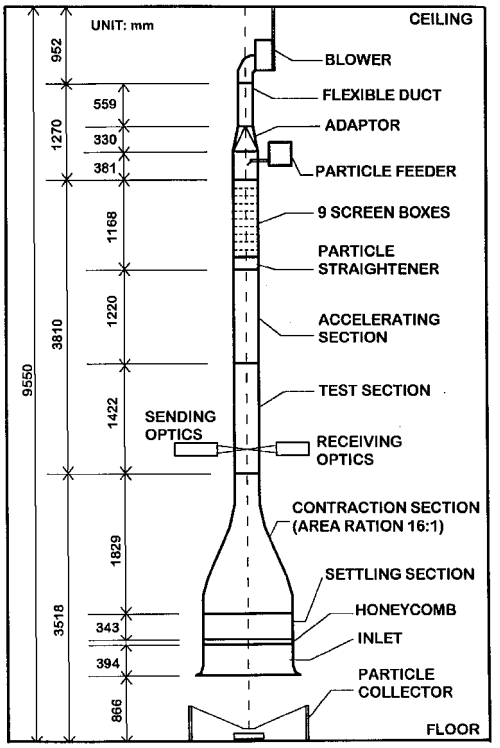

Fig. 1 Counterflow particle/air wind tunnel.

particles in a thin-walled cylindrical container having a 25-mm diameter that was closed at the bottom. The container was mounted on a rod so that it could be traversed across the test section. The accuracy of these measurements was dominated by finite sampling times that were selected to keep experimental uncertainties (95% confidence) less than 10%.

Gas and particle velocities were measured using a traversible (5-μm accuracy) laser velocimetry (LV) system. The LV was based on the 514.5-nm line of an argon-ion laser having an optical power of 1900 mW. A single-channel, dual-beam, forward- scatter, frequency-shifted LV arrangement was used, finding streamwise and cross stream velocities by rotating the optics accordingly. For gas velocities, the sending optics included a 3.75:1 beam expander to yield a measuring volume diameter and length of 55 and 425 μm, respectively. Because of the small measuring volume, the frequency of test particles passing through the measuring volume was small; the few that were observed were readily detected and eliminated from the sample due to their large signal amplitudes and relatively fixed velocities. The airflow entering the wind tunnel was seeded with oil drops having a 1-μm nominal diameter. Velocities were found from the low-pass filtered analog output of a burst-counter signal processor. The combination of frequency shifting plus a constant sampling rate of the analog output of the signal processor eliminated effects of directional bias and ambiguity as well as velocity bias. Temporal power spectra were obtained from the time series of velocities using the FFTRC fast Fourier transform routine.[21] Sampling periods were adjusted to provide the following experimental uncertainties (95% confidence): mean velocities less than 5%, rms velocity fluctuations less than 10%, probability density functions (PDFs) within one standard deviation of the most probable velocity less than 10%, and temporal power spectral densities less than 20% (at frequencies smaller than the reciprocal of the temporal integral scale with uncertainties smaller elsewhere).

Particle velocity measurements were made with the same LV arrangement as the gas velocities except that the optics were changed to provide a larger measuring volume having a diameter of 1.5 mm and a length of 10 mm. This provided a reasonable sampling rate of particle velocities. Optics were rotated to measure streamwise and cross stream velocities. The gas was not seeded for the particle velocity measurements, and the large-amplitude signals from particles were easily separated from background signals due to dust in the air. Sampling periods were adjusted to provide experimental

Table 1 Summary of test conditions[a]

Parameter	Nominal particle diameter, mm		
	0.5	1.1	2.2
U_p, mm/s	3370 (280)[b]	5530 (340)	7000 (200)
Re	106 (9)	373 (23)	990 (28)
C_D	1.22	0.79	0.54
$(dU_p/dx)/U_p$, %/m	2	11	14
$\dot{n}''$, kpart/m^{2}s	71–950	4–56	0.5–10
ℓ_p, mm	32–13	97–41	208–77
L_u, mm	35–11	178–43	156–24
ε, m^2/s^3	0.088–1.17	0.041–0.54	0.012–0.23
ℓ_K, mm	0.5–0.2	0.6–0.3	0.7–0.4
t_K, ms	14–4	20–5	37–8
u_K, mm/s	34–66	28–54	21–44
$\bar{u}'/U_p$, %	0.5–5.0	0.2–0.9	0.2–0.8
$\bar{v}'/U_p$, %	0.5–1.3	0.2–1.2	0.2–0.9

[a]Round glass beads (density of 2500 kg/m^3) falling in upflowing air at standard temperature and pressure (air density of 1.16 kg/m^3 and kinematic viscosity of 15.9 mm^2/s) having a mean velocity of 1.1 m/s. Parameter ranges for each particle size given in order of lowest–highest particle number fluxes, respectively.
[b]Standard deviations given in parentheses.

uncertainties less than 5% for streamwise mean velocities and less than 10% for rms streamwise and cross stream velocity fluctuations. Mean cross stream velocities were nearly zero and only were order of magnitude accurate due to their small magnitudes.

Test conditions are summarized in Table 1. The particles were nearly monodisperse with Reynolds numbers of 106–990, which is representative of the intermediate-Reynolds-number conditions of drops in sprays.[15] Terminal velocities and drag coefficients were measured, yielding values that agreed with the standard drag curve for spheres due to Putnam[22] within 15%. Test conditions were adjusted so that turbulence intensities relative to the mean gas velocity were less than 15% so that LV measuring conditions were excellent and the use of Taylor's hypothesis to convert temporal to spatial spectra and scales was justified.[23] The particles approached but did not reach terminal velocity conditions during the present turbulence generation measurements (e.g., rates of particle acceleration at the measuring location were in the range 2–14% of mean relative particle velocities per meter), whereas mean cross stream particle velocities were small. Particle velocity fluctuations were small due to their poor response to air motion and were mainly caused by variation of particle sizes.

Assuming that the particles are falling randomly, the mean particle spacing can be found from

$$\ell_p = [(U_p - \bar{u})/\dot{n}'']^{\frac{1}{3}} \tag{1}$$

which yields values of 13–208 mm and particle volume fractions less than 0.003% for the present experiments. Measured streamwise integral length scales had magnitudes comparable to mean particle spacings and were in the range 11–178 mm. The direct dissipation of turbulence kinetic energy (dissipation) by particles is less than 4% for present test conditions.[20] Thus, dissipation can be equated to the rate of turbulence generation by particles, which in turn is equal to the rate of transfer of mechanical energy to the gas as the particles move through the flow, that is,

$$\varepsilon = \pi \dot{n}'' d_p^2 C_D U_p^2 \left| \right. 8 \tag{2}$$

Given ε, the Kolmogorov scales can be computed from their definitions,[19] yielding the ranges summarized in Table 1. Relative turbulence intensities due to turbulence generation were in the range 0.2–5.0%.

Results and Discussion

Apparatus Evaluation

The temporal and spatial uniformity of the particle flows were evaluated by collecting samples for various time periods and by traversing the sampling probe along the two perpendicular axes of symmetry at the lowest cross section, where measurements were made. These measurements were carried out for all three particle sizes, spanning present ranges of particle fluxes for each size. Samples obtained from multiples of the shortest sampling period showed that the particle fluxes were statistically stationary with sampling times extending up to roughly 1000 times typical temporal integral scales of the present flows. Finally, the sampling measurements showed that mean particle fluxes varied less than 10% over the central 205 × 205 mm cross section of the flow, where velocity measurements were made. Mean and fluctuating particle velocities were also uniform within experimental uncertainties over the same region. The properties of the continuous (gas) phase were established by measurements of mean and fluctuating streamwise velocities at various times and over the central 205 × 205 mm cross section of the flow, considering streamwise distances up to ±100 mm from the normal cross section, where measurements were made. These results were not affected significantly for upflow velocities of 500–1300 mm/s. At these conditions, gas flow properties were statistically stationary and homogeneous within experimental uncertainties. See Ref. 20 for plots of all of the apparatus evaluation measurements.

Measurements of streamwise velocities for various particle sizes, particle fluxes, and upflow velocities were also used to establish minimum allowable particle fluxes. In particular, very low particle fluxes for a given upflow velocity yielded homogeneous flows having spurious turbulence intensities, amounting to relative turbulence intensities of 0.1–0.2% depending on particle size, due to inlet disturbances of the wind tunnel. Increasing the particle flux disrupted these disturbances and caused relative turbulence intensities to decrease for a time as particle fluxes increased before increasing once again in a manner similar to the behavior of turbulence generation seen in Refs. 6 and 7; therefore, present measurements were only undertaken for particle fluxes somewhat larger than the minimum relative turbulence intensity condition. Relative turbulence intensities at low particle fluxes were also affected by the upflow velocity. An upflow velocity of 1.1 m/s was finally selected to maximize the range of particle fluxes that could be considered while avoiding the excessive particle concentrations in the flow that are observed when upflow velocities approach the terminal velocity of the particles [see Eq. (1)]. For these conditions turbulence levels of the particle-laden flows ranged from twice to two orders of magnitude larger than the unladen flow, and it is unlikely that wind-tunnel disturbances affected the results reported here.

Particle Wake Properties

Typical temporal records of streamwise and cross stream gas velocities are illustrated in Fig. 2. When interpreting these data, it should be recalled that streamwise and cross stream velocities were observed at different times and there is no correlation between the two. In addition, the plots have low resolution to show the general appearance of the data over a sufficiently long period of time (50 s) so that several wake disturbances can be seen, even for the smallest particle number flux shown. Results are illustrated for all three particle sizes, characterized both by the particle number flux and the dimensionless dissipation factor of Refs. 6 and 7.

The most obvious features of the streamwise velocities illustrated in Fig. 2 is the appearance of relatively large negative velocity disturbances (negative velocity spikes) protruding from the smaller amplitude irregular turbulentlike background velocity signal. The frequency of appearance of these spikes is seen to increase as the particle number flux increases. Observations for long periods of time showed that the maximum velocity disturbances of these spikes were comparable to values expected based on the relative particle velocities for each particle size summarized in Table 1 (Note that the spikes illustrated in Fig. 2 have smaller magnitudes representative of far wake conditions that are most frequently observed; subsequent results will address near-wake conditions.) Thus, these spikes are associated with flow properties within particle wake disturbances.

Other properties of the velocity records illustrated in Fig. 2 suggest wake behavior similar to the laminarlike turbulent wakes observed in Refs. 16 and 17. For example, results for the 0.5-mm particles ($Re = 106$) exhibit negative spikes in the streamwise direction but no spikes in the cross stream direction. This behavior is consistent with laminarlike turbulent wake behavior at this value of Reynolds number, however, because mean cross stream velocities

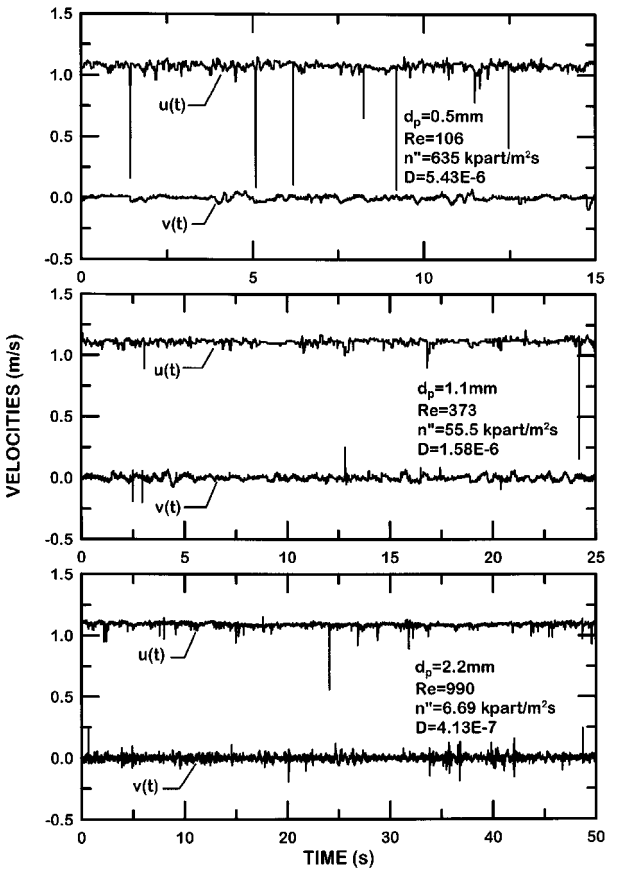

Fig. 2 Effect of particle loading and size on streamwise and cross stream velocity records.

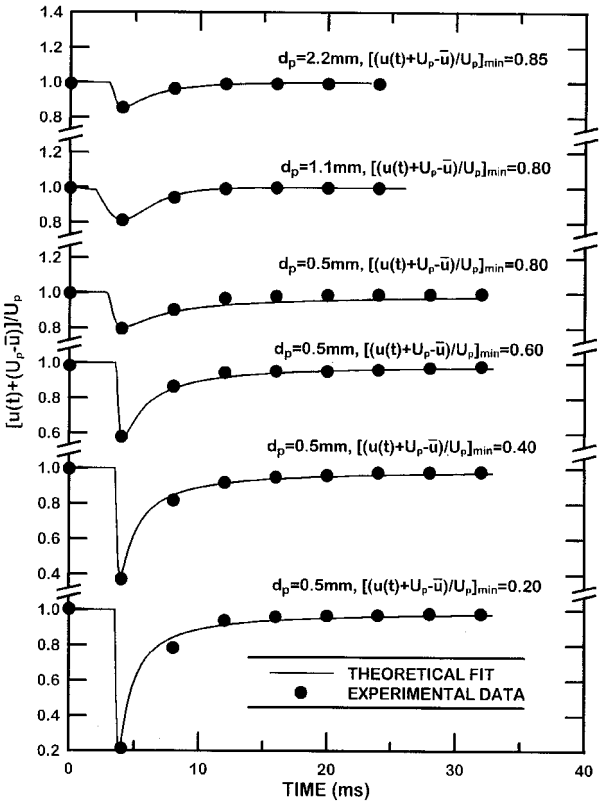

Fig. 3 Measured and predicted streamwise velocities in particle wakes as a function of time for various velocity defects and particle sizes.

are small compared to both mean streamwise velocities and rms velocity fluctuations in laminarlike turbulent wakes and only the streamwise rms velocity fluctuations are observed before eddy shedding starts at $Re \approx 300$ (Refs. 16 and 17). In contrast, both large negative velocity spikes in the streamwise direction and spikes having both positive and negative velocity disturbances in the cross stream direction are observed for the 1.1- and 2.2-mm-diam particles that have $Re = 373$ and 990, respectively. This behavior is exactly what should be observed for laminarlike turbulent wakes, however, because cross stream turbulent velocity fluctuations are comparable to streamwise mean velocity defects when eddy shedding occurs for $Re > 300$ (Refs. 16 and 17).

The extended regions between wake disturbances in Fig. 2 exhibit turbulentlike behavior representative of the turbulent interwake region. The amplitudes of the velocity fluctuations in the turbulent interwake region do not vary significantly with time but tend to increase as the dissipation factor increases. The relationship between rms velocity fluctuations in the turbulent interwake region and the dissipation factor will be quantified later.

A final assessment of the similarities between the wake disturbances observed during the present turbulence generation studies and the laminarlike turbulent wakes observed in Refs. 16 and 17 involved direct comparison of mean streamwise velocities. This comparison was carried out for all three particle sizes at relatively large particle loadings so that representative samples of particle wakes could be observed in reasonable test times. Measurements were made for various maximum velocity defects, which represent results for paths of the LV measuring volume at various radial distances from the wake axis, because present particle paths were essentially vertical and the maximum mean velocity defect is a monotonic function of radial distance from the wake axis for laminarlike turbulent wakes.[16,17,20] Effects of turbulence were handled by averaging several velocity records (selected to have a maximum velocity defects within ±25% of the given maximum velocity defect) to obtain an estimate of mean streamwise wake velocities [the averaging criterion was an experimental uncertainty (95% confidence) of the maximum mean velocity defect less than 10%]. Predictions assuming vertical wake axes and having the same maximum mean velocity defects were obtained from the correlations for the mean properties of laminarlike turbulent wakes of Refs. 16 and 17 (at the same particle Reynolds number and relative turbulence intensity).

The resulting measured and predicted mean streamwise velocities in the particle wakes are illustrated in Fig. 3. These results involve plots of normalized streamwise velocities as a function of time for various particle diameters and maximum velocity defects. Note that the normalization of the ordinate of Fig. 3 implies that a value of 0 corresponds to the absolute (negative) particle velocity whereas a value of 1 corresponds to the absolute (positive) mean upflow velocity of the wind tunnel. Results for 0.5-mm particles are relatively comprehensive and involve dimensionless mean velocity defects in the range 0.20–0.80 because sampling rates were relatively large for these small particles. Results for particle diameters of 1.1 and 2.2 mm are limited to a single velocity defect (representative of the outer edge of the wakes) in order to obtain reasonable sampling rates for these small-particle flux conditions. It is evident that the agreement between measurements and predictions is excellent in Fig. 3, which supports the use of the laminarlike turbulent wake properties of Refs. 16 and 17 to help interpret present observations of turbulence generation.

Based on the reported findings, it seems reasonable to assume that the present wake disturbances are similar to the laminarlike turbulent wakes described in Refs. 16 and 17. This information was then used to estimate the proportions of the wake and interwake regions as well as the extent of direct wake/wake interactions. This was done by carrying out stochastic simulations to find realizations of particle positions in space for various particle fluxes and the three particle sizes. Random selections in three dimensions were made while accounting for the slight compression of particle spacing in the vertical direction due to gas upflow as discussed in connection with Eq. (1). Appropriate laminarlike turbulent wakes were then associated with each particle, assuming that wake radii were equal to twice the characteristic wake width at each streamwise distance behind the particle and that the wake extended in the streamwise direction until the maximum mean velocity defect was equal to the

ambient rms streamwise velocity fluctuations. These results indicated that wake cross-sectional areas generally were less than 30% of the available cross-sectional area and that less than 25% of the wakes experienced direct wake-to-wake interactions at any one time (with these interactions mainly confined to conditions far from both particles) over the present test range. Thus, the present flows involve laminarlike turbulent wakes surrounded by a relatively large turbulent interwake region, with occasional wake-to-wake interactions. This view agrees with the velocity traces of Figs. 2 if it is recognized that only a relatively small portion of each wake can generate the large velocity spikes seen on these plots. Further evidence of combined effects of the wake and interwake regions on overall flow properties will be sought from consideration of PDFs and spectra in the following.

PDF

More insight about the effect of particle wake disturbances on the total turbulence properties of homogeneous dispersed flows dominated by turbulence generation can be obtained from the PDFs of velocity fluctuations. Typical results along these lines are presented in Figs. 4 and 5 for 2.2- and 0.5-mm particles, respectively, which bound results for 1.1-mm particles. On each of these plots, PDFs are shown for streamwise and cross stream velocities at the low and high particle loadings specified by the dissipation factor values. Fits of the measurements are also shown on the plots, corresponding to least-squares sectional fits for the PDF(u) and best Gaussian fits for the PDF(v). The best Gaussian fits were established from the measured mean and rms fluctuating values obtained during the corresponding measurements.

The present PDFs plotted in Figs. 4 and 5 do not agree with earlier observations of Refs. 6 and 7 for dispersed flows in stagnant baths, which yielded Gaussian PDFs for both velocity components, with at most a slight upward bias (roughly 10% when averaged over all test conditions) of the PDF(u) near its most probable value. This behavior agrees with present behavior of PDF(v), which is nicely fitted by Gaussian PDFs for both loadings of all particle sizes. In contrast, the present PDF(u) are more peaked and somewhat skewed toward negative velocities compared to the mean velocity, that is, the PDF(u) exhibit greater kurtosis and skewness than the nearly Gaussian PDF(v) (Ref. 19). In addition, the PDF(u) for each

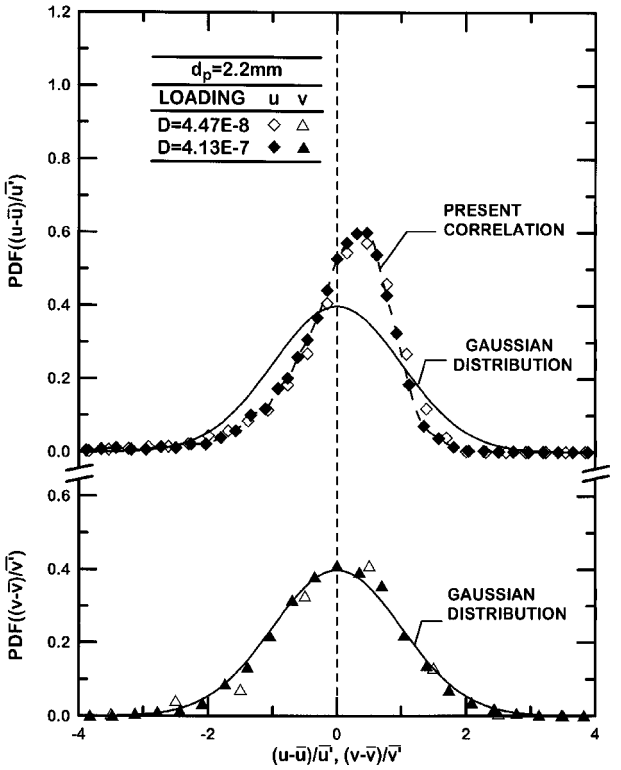

Fig. 4 Streamwise and cross stream velocity PDFs at various particle loadings for 2.2-mm particles.

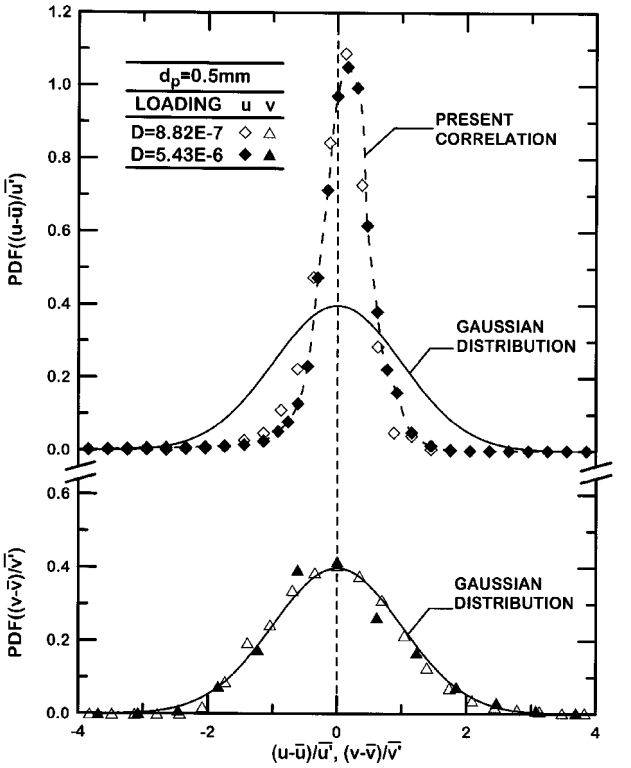

Fig. 5 Streamwise and cross stream velocity PDFs at various particle loadings for 0.5-mm particles.

particle size tends to be independent of particle loading, similar to PDF(v), but the PDF(u) becomes progressively more peaked (or has progressively increasing kurtosis) as the particle size (or Reynolds number) decreases. All of these characteristics can be explained from the properties of the streamwise and cross stream velocity records (and the spike disturbances due to particle wakes seen in the velocity records) of Figs. 2 and 3, as discussed next.

The main reason for the different PDF(u) of Refs. 6 and 7 and the present study follows from the much improved LV conditions of the present study that allowed the near-wake region of the spike disturbances due to particle wakes seen in Fig. 3 to be resolved for the streamwise velocity records. This point was easily demonstrated during the present experiments by reducing seeding levels so that the spikes seen in Fig. 2 were rarely resolved; the corresponding PDF(u) then became more Gaussian, similar to the results of Refs. 6 and 7. The other properties of PDF(u) in Figs. 4 and 5 then follow from the well-known effects of the properties of the velocity signal on the values of the skewness and kurtosis of the PDF(u). In particular, the spikes always contribute a streamwise negative velocity signal based on the results illustrated in Fig. 2; this implies a corresponding positive bias of the PDF(u), or negative skewness.[19] The more rapid reduction of streamwise velocities in the radial direction for small d_p (or Reynolds number) conditions (yielding narrower wake disturbances) implies a more peaked PDF(u), or a larger kurtosis of the PDF(u), for similar reasons.[19] In addition, the small effect of particle flux on the PDF(u) and the PDF(v) is consistent with the generally observed behavior of these functions, where the shape of the velocity signal as a function of time affects the skewness and kurtosis of the PDF but not the characteristic frequency of the signal,[19] for example, homogeneous, isotropic dispersed flows have Gaussian PDFs irrespective of their characteristic timescales or frequency scales. Finally, either the absence of discernible spikes for the cross stream velocity records for the 0.5-mm particles or the presence of both positive and negative spikes due to wake turbulence for the cross stream velocity records for the 2.2 mm particles is entirely consistent with the Gaussian behavior of the PDF(v) seen in Figs. 4 and 5. Taken together, the combined findings of Figs. 2–5 suggest that both particle wake disturbances and the interwake region provide significant contributions to the overall apparent turbulence properties of the present turbulence generated flows.

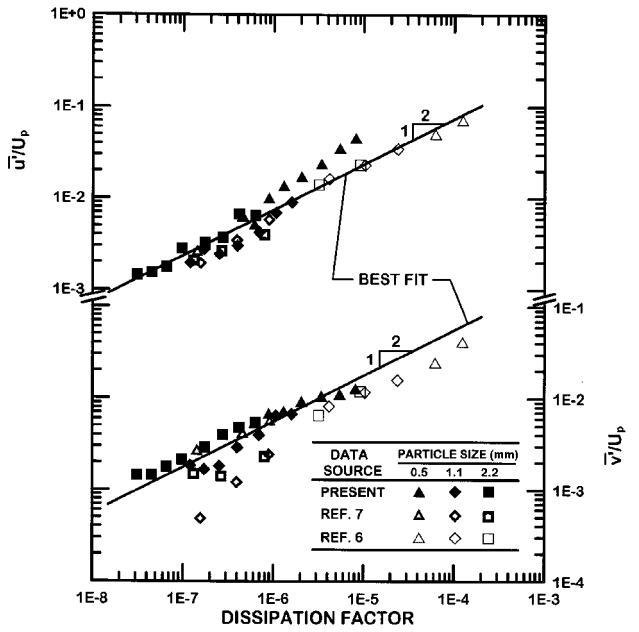

Fig. 6 Streamwise and cross stream rms velocity fluctuations as a function of particle dissipation factors and diameters: measurements of Parthasarathy and Faeth,[6] Mizukami et al.[7] and the present investigation.

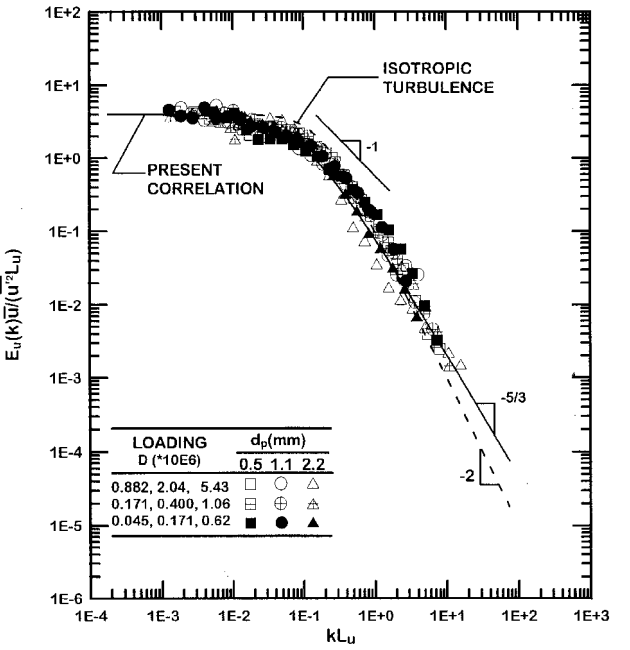

Fig. 7 Energy spectra of streamwise velocity fluctuations for various particle loadings and sizes.

Velocity Fluctuations

The measurements of velocity fluctuations in Refs. 6 and 7 were correlated based on an approximate stochastic approach assuming that velocity fluctuations were entirely due to wake disturbances. This approach yielded reasonably effective correlations of relative turbulence intensities of streamwise and cross stream velocity fluctuation in terms of a dissipation factor D resulting from the approximate stochastic theory. This approach will be considered in the following due to its past success.

Measurements of streamwise and cross stream relative turbulence intensities are plotted as a function of the dissipation factor in Fig. 6. Measurements shown in Fig. 6 include results for particles in still (in the mean) water due to Parthasarathy and Faeth,[6] results for particles in still (in the mean) air due to Mizukami et al.,[7] and the present results for particles in counterflowing air. All three experiments used the same 0.5-, 1.1-, and 2.2-mm spherical glass particles. Correlations in terms of $D^{1/2}$, as suggested by the stochastic theory of Ref. 6, are fitted to the combined data sets for each velocity component. The correlations are seen to provide only fair agreement with the measurements. This is particularly true for the measurements of Mizukami et al.,[7] which exhibit significant scatter when plotted in the manner of Fig. 6. The results suggest some relationship between the properties of the wakes and the interwake region but clearly a correlation solely in terms of D cannot capture features such as the onset of cross stream wake disturbances for $Re > 300$ seen in Fig. 2. Thus, the correlations illustrated in Fig. 6 are only tentative pending more information about flow properties in the interwake region and the use of these results in a more rational conditional averaging procedure to summarize the properties of flows caused by turbulence generation.

Energy Spectra

Taylor's hypothesis could be used to convert measured temporal power spectra and temporal integral scales into energy spectra and spatial integral scales because present absolute turbulence intensities were small.[23] The resulting streamwise energy spectra are plotted as functions of normalized wave numbers in Fig. 7. Results are shown for various particle sizes and fluxes, with the latter represented by values of the dissipation factor. The LV conditions for these measurements were good so that effects of step noise were deferred until Kolmogorov wave numbers were approached. (This condition roughly corresponds to $kL_u = 100$.) The values of L_u for the measurements were found by setting $E_u(k)\bar{u}/(\bar{u}'^2L_u) = 4$ as kL_u becomes small, as discussed by Hinze.[23] A correlation of the energy spectra for approximate isotropic turbulence is also shown on the plot, for comparison with the present measurements. This correlation represents a simplification of isotropic turbulence, where the $-\frac{5}{3}$ power decay of the inertial range is approximated by a -2 power decay that corresponds to an exponential temporal correlation of streamwise velocity fluctuations.[23] The energy spectra provide reasonably good correlations of present measurements as plotted in Fig. 7.

An interesting feature of the spectra of Fig. 7 is that they decay over a rather large range of kL_u (roughly four decades) even though present particle Reynolds numbers are not large (less than 1000). Much of this behavior is typical of other homogeneous turbulence fields where disturbances due to grids (having relatively small grid element Reynolds numbers) yield turbulent flows having extensive inertial ranges.[4,19,23] Another feature of the present flows enhances this behavior, however, as pointed out in earlier work.[6,7] In particular, the spectra of Fig. 7 include contributions from both particle wake disturbances and the turbulent interwake region. Then because the wake arrivals are random, mean velocities in the wakes contribute to the spectra increasing the range of scales that are present. Naturally, similar contributions are not present for grid-generated turbulence because measurements of these flows are made well downstream of the region of significant direct wake disturbances from the turbulence-generating grid.

The energy spectra of Fig. 7 also provide other evidence of direct contributions of mean velocities in wake disturbances. In particular, the spectra exhibit prominent -1 and $-\frac{5}{3}$ decay regions as kL_u increases. The -1 power decay region is not seen in conventional turbulent flows, but based on the approximate stochastic analysis of Ref. 6 such behavior is typical of the contribution of mean velocities in wake disturbances to temporal power spectra (and thus energy spectra under present approximations). Other evidence for this explanation is that the -1 decay region is associated with values of kL_u on the order of unity (which is roughly approximated by $k\ell_p$ in the order of unity; see Table 1) that is characteristic of wake dimensions. Larger wave numbers exhibit $-\frac{5}{3}$ power decay regions that are representative of conventional turbulence and probably involve contributions from both the wake disturbances and the turbulent interwake region as discussed earlier in connection with Fig. 2.

Conclusions

This investigation considered the properties of homogeneous turbulence generated by uniform fluxes of monodisperse spherical

particles moving through air at standard temperature and pressure. The experimental configuration consisted of particles falling in counterflowing air to supplement earlier measurements for particles falling in stagnant water (Ref. 6) and stagnant air (Ref. 7). Present test conditions included particle Reynolds numbers of 106–990, particle volume fractions less than 0.003% and direct rates of dissipation of turbulence by particles less than 4%, and particle number fluxes sufficient to yield relative turbulence intensities of 0.2–5%. The major conclusions of the study are as follows.

1) Measurements of gas velocities indicate that the particle wake properties of the present turbulence-generation processes correspond to the laminarlike turbulent wakes observed in Refs. 16 and 17 for spheres at intermediate Reynolds numbers in isotropic turbulence.

2) Estimates of the character of the present flows based on the properties of laminarlike turbulent wakes suggest that wake disturbances (generally involving cross-sectional areas less than 30% of the total available cross-sectional area) are embedded in a relatively large turbulent interwake region with relatively few (less than 25%) direct wake-to-wake interactions, with the latter dominated by portions of the wakes far from both particles.

3) Present measurements of relative turbulence intensities were in fair agreement with earlier measurements of turbulence generation in still liquids and gases from Refs. 6 and 7, and all of these measurements could be correlated in terms of the dissipation factor. These correlations are only considered tentative, however, pending development of a more rational approach that properly accounts for the relative contributions of wake disturbances and the turbulent interwake region, which fundamentally have very different flow properties.

4) Other properties measured during the present study, PDFs and spectra, were not in good agreement with the earlier observations of Refs. 6 and 7. In particular, present observations provided direct evidence of effects of both wake disturbances and interwake regions (as non-Gaussian PDFs and prominent -1 and $-\frac{5}{3}$ decay regions of energy spectra) that were either absent or less evident during the earlier studies. These differences were shown to result from the improved LV measuring conditions of the present study.

5) Contributions from both the wake disturbances and the turbulent interwake region also were responsible for the surprisingly large range of scales seen in the present flows in spite of relatively small particle Reynolds numbers. In particular, mean velocities in particle wake disturbances contribute to present apparent turbulence properties because wake arrivals are random and this contribution is generally not present in turbulence generated in other ways, for example, by grids or shear flows.

Acknowledgments

This investigation was supported by the Air Force Office of Scientific Research, Grants F49620-92-J-0399, F49620-95-I-0364, and F49620-99-1-0083, under the technical management of J. M. Tishkoff.

References

[1]Hinze, J. O., "Turbulent Fluid and Particle Interaction," *Progress in Heat and Mass Transfer*, Vol. 6, 1972, pp. 433–452.

[2]Hetsroni, G., "Particles-Turbulence Interaction," *International Journal of Multiphase Flow*, Vol. 15, No. 5, 1989, pp. 735–746.

[3]Squires, K. D., and Eaton, J. K., "Particle Response and Turbulence Modification in Isotropic Turbulence," *Physics of Fluids A*, Vol. 2, No. 6, 1990, pp. 1191–1203.

[4]Rogers, C. B., and Eaton, J. K., "The Effect of Small Particles on Fluid Turbulence in a Flat-Plate Turbulent Boundary Layer in Air," *Physics of Fluids A*, Vol. 3, No. 5, 1991, pp. 928–937.

[5]Parthasarathy, R. N., and Faeth, G. M., "Structure of Particle-Laden Turbulent Water Jets in Still Water," *International Journal of Multiphase Flow*, Vol. 13, No. 5, 1987, pp. 699–716.

[6]Parthasarathy, R. N., and Faeth, G. M., "Turbulence Modulation in Homogeneous Dilute Particle-Laden Flows," *Journal of Fluid Mechanics*, Vol. 220, Pt. 2, 1990, pp. 485–514.

[7]Mizukami, M., Parthasarathy, R. N., and Faeth, G. M., "Particle-Generated Turbulence in Homogeneous Dilute Dispersed Flows," *International Journal of Multiphase Flow*, Vol. 18, No. 2, 1992, pp. 397–412.

[8]Gore, R. A., and Crowe, C. T., "Effect of Particle Size on Modulating Turbulent Intensity," *International Journal of Multiphase Flow*, Vol. 15, No. 2, 1989, pp. 279–285.

[9]Kenning, V. M., and Crowe, C. T., "On the Effect of Particles on Carrier Phase Turbulence in Gas-Particle Flows," *International Journal of Multiphase Flow*, Vol. 23, No. 2, 1997, pp. 403–408.

[10]Yuan, Z., and Michaelides, E., "Turbulence Modulation in Particulate Flows—A Theoretical Approach," *International Journal of Multiphase Flow*, Vol. 18, No. 5, 1992, pp. 779–785.

[11]Rashidi, M., Hetsroni, G., and Banerjee, S., "Particle-Turbulence Interaction in a Boundary Layer," *International Journal of Multiphase Flow*, Vol. 16, No. 6, 1990, pp. 935–949.

[12]Lance, M., and Bataille, J., "Turbulence in the Liquid Phase of a Uniform Bubbly Air–Water Flow," *Journal of Fluid Mechanics*, Vol. 222, Pt. 1, 1991, pp. 95–119.

[13]Rice, S. O., "Mathematical Analysis of Random Noise," *Noise and Stochastic Processes*, edited by N. Wax, Dover, New York, 1954, pp. 133–294.

[14]Batchelor, G. K., "Sedimentation in a Dilute Dispersion of Spheres," *Journal of Fluid Mechanics*, Vol. 52, 1971, pp. 245–268.

[15]Wu, J.-S., and Faeth, G. M., "Sphere Wakes in Still Surroundings at Intermediate Reynolds Numbers," *AIAA Journal*, Vol. 31, No. 8, 1993, pp. 1448–1455.

[16]Wu, J.-S., and Faeth, G. M., "Sphere Wakes at Moderate Reynolds Numbers in a Turbulent Environment," *AIAA Journal*, Vol. 32, No. 3, 1994, pp. 535–541.

[17]Wu, J.-S., and Faeth, G. M., "Effects of Ambient Turbulence Intensity on Sphere Wakes at Intermediate Reynolds Numbers," *AIAA Journal*, Vol. 33, No. 1, 1995, pp. 171–173.

[18]Schlichting, H., *Boundary Layer Theory*, 7th ed., McGraw–Hill, New York, 1979, pp. 234, 235, 599.

[19]Tennekes, H., and Lumley, J. L., *A First Course in Turbulence*, MIT Press, Cambridge, MA, 1972, pp. 113–124, 196–201.

[20]Chen, J.-H., "Turbulence Generation in Homogeneous Dilute Particle-Laden Flows," Ph.D. Dissertation, Dept. of Aerospace Engineering, Univ. of Michigan, Ann Arbor, MI, May 1999.

[21]*IMSL Library Reference Manual*, 8th ed., IMSL, Inc., Houston, TX, 1980.

[22]Putnam, A., "Integrable Form of Droplet Drag Coefficient," *ARS Journal*, Vol. 31, No. 10, 1961, pp. 1467, 1468.

[23]Hinze, J. O., *Turbulence*, 2nd ed., McGraw–Hill, New York, 1975, Chap. 3, p. 204.

S. K. Aggarwal
Associate Editor